Colloquia: LaThuile15

Measurement of A_{FB} in $B^{\pm}$ meson production at D0

J. Hogan on behalf of the D0 Collaboration

Rice University - Houston, TX, USA

Summary. — We present a measurement of the forward-backward asymmetry in the production of $B^{\pm}$ mesons, $A_{\mathrm{FB}}(B^{\pm})$, using $B^{\pm} \to J/\psi K^{\pm}$ decays in 10.4 fb^{-1} of $p\bar{p}$ collisions at $\sqrt{s} = 1.96$ TeV collected by the D0 experiment during Run II of the Tevatron collider. A nonzero asymmetry would indicate a preference for a particular flavor, *i.e.*, b quark or $\bar{b}$ antiquark, to be produced in the direction of the proton beam. We extract $A_{\mathrm{FB}}(B^{\pm})$ from a maximum-likelihood fit to the difference between the numbers of forward- and backward-produced $B^{\pm}$ mesons. We measure an asymmetry consistent with zero: $A_{\mathrm{FB}}(B^{\pm}) = [-0.24 \pm 0.41\,(\text{stat}) \pm 0.19\,(\text{syst})]\%$.

PACS `13.25.Hw` – Decays of bottom mesons.
PACS `11.30.Er` – Charge conjugation, parity, time reversal, and other discrete symmetries.

Over the few past years there has been much interest in the forward-backward asymmetry in $t\bar{t}$ production ($A_{\mathrm{FB}}^{t\bar{t}}$) [1], especially since initial experimental results were larger than standard model (SM) predictions [2,3]. These observations prompted development of models beyond the SM that could explain the excess [4]. The corresponding asymmetry in $b\bar{b}$ production, $A_{\mathrm{FB}}^{b\bar{b}}$, has the same sources as $A_{\mathrm{FB}}^{t\bar{t}}$ but is expected to have a smaller magnitude in the SM, making it an important probe of these new physics models [5,6].

The most recent D0 measurements of $A_{\mathrm{FB}}^{t\bar{t}}$ [7] agree with the SM [8]. A closely related quantity called the $t\bar{t}$ charge asymmetry has been studied at the LHC [9,10]. The LHCb collaboration has recently measured the charge asymmetry between b and $\bar{b}$ jets in pp collisions [11].

A forward-backward asymmetry in the production of heavy quark Q is primarily caused by interference between tree-level and loop diagrams for $q\bar{q} \to Q\bar{Q}$ interactions, and also by interference between initial and final state gluon radiation [13]. We measure the forward-backward asymmetry [12] using fully reconstructed $B^{\pm} \to J/\psi(\to \mu^{+}\mu^{-})K^{\pm}$ decays where the $B^{\pm}$ directly identifies the quark flavor (*i.e.*, b or $\bar{b}$). Compared to b jet reconstruction, this method has the advantages that the charge of the b quark is unambiguously determined, and there is no need to account for $B^{0}/\bar{B}^{0}$ oscillations. The quantity $A_{\mathrm{FB}}(B^{\pm})$ is sensitive to the same production asymmetries as $A_{\mathrm{FB}}^{b\bar{b}}$. In $p\bar{p}$

collisions, the forward category indicates a $b\,(\bar{b})$ quark, or $B^-\,(B^+)$ meson, emitted with a longitudinal momentum component in the direction of the proton (antiproton) beam.

We reconstruct a $B^\pm$ meson and categorize it as forward or backward with a variable $q_{\mathrm{FB}} = -q_B\,\mathrm{sgn}(\eta_B)$, where q_B is the $B^\pm$ meson electric charge, $\mathrm{sgn}(x)$ is the sign function, and η_B is the $B^\pm$ meson pseudorapidity. Pseudorapidity is defined as $\eta = -\ln[\tan(\theta/2)]$, where θ is the laboratory frame polar angle with respect to the proton beam direction. The forward-backward asymmetry of the $B^\pm$ mesons is

$$(1) \qquad A_{\mathrm{FB}}(B^\pm) = \frac{N(q_{\mathrm{FB}} > 0) - N(q_{\mathrm{FB}} < 0)}{N(q_{\mathrm{FB}} > 0) + N(q_{\mathrm{FB}} < 0)}.$$

Inclusive predictions of $A_{\mathrm{FB}}^{b\bar{b}}$ give positive asymmetries of $\approx 0.5\%$ [5, 14], but the mass scales of the $b\bar{b}$ pairs considered $[M(b\bar{b}) > 35\,\mathrm{GeV}$, or $p(b) > \approx 15\,\mathrm{GeV}]$ are more relevant for a jet-based analysis. To make SM predictions tailored to our kinematics and selections, we produce next-to-leading-order Monte Carlo (MC) samples for QCD production of $B^\pm$ in the process $p\bar{p} \to b\bar{b}X$. MC events are generated using MC@NLO [15] with parton distribution function (PDF) set CTEQ6M1 [16] and HERWIG [17] for parton showering and hadronization. Detector simulation is performed using GEANT3 [18]. Since our publication, a SM calculation for this process has been performed giving $A_{\mathrm{FB}}^{\mathrm{SM}}(B^\pm) = (0.021 \pm 0.008)\%$ [19].

The D0 experiment collected data at $\sqrt{s} = 1.96\,\mathrm{TeV}$ during Run II of the Fermilab Tevatron $p\bar{p}$ collider, from 2002 until the Tevatron shutdown in 2011. The D0 detector is described in detail elsewhere [20]. We define a coordinate system with the z-axis along the proton beam direction, the x-axis pointing away from the Tevatron center, and the y-axis pointing upwards. For this analysis the most important detector elements are the central tracking and muon systems. The central tracking system consists of a silicon microstrip tracker and a central fiber tracker, both located within a 1.9 T superconducting solenoidal magnet, with designs optimized for tracking and vertex finding at pseudorapidities $|\eta| < 3$ and $|\eta| < 2.5$, respectively. The muon system has a layer of tracking detectors and scintillation trigger counters outside a liquid argon sampling calorimeter and two similar layers outside a 1.8 T iron toroid [21], and covers the region $|\eta_{\mathrm{det}}| \approx 2$ where $|\eta_{\mathrm{det}}|$ is measured from the center of the detector. The solenoid and toroid magnet polarities were reversed approximately every two weeks giving nearly equal beam exposure to each polarity combination. The data used in this analysis were collected with a suite of single muon and dimuon triggers.

We select $B^\pm \to J/\psi K^\pm$ candidates from the D0 Run II data set with an integrated luminosity of $10.4\,\mathrm{fb}^{-1}$. Candidates are reconstructed by identifying a pair of oppositely charged muons (decay products of the J/ψ meson) produced along with a charged track (the $K^\pm$ candidate) at a common vertex displaced from the $p\bar{p}$ interaction vertex.

All tracks must lie within the pseudorapidity coverage of the muon and central tracking systems, $|\eta| < 2.1$. Selected muons have transverse momentum $p_T > 1.5\,\mathrm{GeV}$, and $K^\pm$ candidates have $p_T > 0.7\,\mathrm{GeV}$. At least one muon must traverse both inner and outer layers of the muon detector. Both muons must match to tracks in the central tracking system. The J/ψ candidates with reconstructed invariant mass $M(\mu^+\mu^-)$ between 2.7 and 3.45 GeV are accepted if their transverse decay length (L_{xy}) uncertainty is less than 0.1 cm, where L_{xy} is the distance from the $p\bar{p}$ vertex to a particle's decay vertex in the x-y plane. The cosine of the pointing angle, defined as the angle between a particle's

momentum vector and the vector from the $p\bar{p}$ vertex to the particle's decay vertex, must be greater than zero.

The combination of μ^+, μ^-, and $K^{\pm}$ tracks to form a $B^{\pm}$ decay vertex must have $\chi^2 < 16$ for 3 degrees of freedom, and the cosine of the $B^{\pm}$ pointing angle must be above 0.8. $B^{\pm}$ candidates are accepted if they are significantly displaced from the $p\bar{p}$ vertex. Their transverse decay length significance (defined as L_{xy} divided by its uncertainty) must be greater than three. To calculate the $B^{\pm}$ candidate mass we correct the muon momenta by constraining $M(\mu^+\mu^-)$ to the world average J/ψ meson mass [22]. The selected $B^{\pm}$ mass range is 5.05–5.65 GeV.

Because definitions of forward and backward are tied directly to $\mathrm{sgn}(\eta_B)$, the ambiguous region near $\eta_B = 0$ is given special consideration. We compare η of the $B^{\pm}$ mesons and their parent b quarks at the production and reconstruction levels in MC@NLO. Rejecting events with $|\eta_B| < 0.1$ removes all $B^{\pm}$ mesons reconstructed with incorrect q_{FB} without significantly affecting $A_{\mathrm{FB}}(B^{\pm})$. After the cut, more than 99.9% of $B^{\pm}$ mesons give the same q_{FB} as the parent b quark, indicating minimal hadronization effects on $A_{\mathrm{FB}}(B^{\pm})$. The distribution of $(\eta_b - \eta_B)$ has a rms width of 0.11.

Background rejection is improved using a boosted decision tree (BDT) [23] trained on a simulated MC signal sample and a background sample from data sidebands around the selected $B^{\pm}$ mass range (4.0–5.05 and 5.65–7.0 GeV). Leading-order signal MC events are generated with PYTHIA [24] and processed through the same reconstruction code used for data. We weight MC events so that the p_T distributions of the muons match the distributions in data, which are affected by trigger inefficiencies. Additional weights are applied to match distributions of $p_T(B^{\pm})$, $p_T(K^{\pm})$, and χ^2 of the $B^{\pm}$ decay vertex fit to data distributions. Finally, we weight MC events so that the probability of reconstructing isolated muons or $B^{\pm}$ candidates matches the probability measured in data. Isolated particles have no other tracks in a cone of size $\Delta\mathcal{R} = 1$ around them, where ϕ is the azimuthal angle in the x-y plane, and $\Delta\mathcal{R} = \sqrt{\Delta\phi^2 + \Delta\eta^2}$ is the angular separation between tracks. This weighting gives optimal agreement between data and simulation in all 40 BDT input variables, which include particle momenta, distances from the $p\bar{p}$ vertex, decay lengths, pointing angles, isolation of the muons and $B^{\pm}$ meson, and azimuthal angle separation for various particle pairs. A cut on the BDT discriminant is chosen to minimize the statistical uncertainty of $A_{\mathrm{FB}}(B^{\pm})$. After all cuts we find one $B^{\pm}$ candidate in 98.5% of events, with the remainder having two or more candidates. All candidates are used independently in this analysis.

We extract $A_{\mathrm{FB}}(B^{\pm})$ from a maximum-likelihood fit incorporating a signal probability distribution and three background distributions (see below), which are functions of the reconstructed $B^{\pm}$ mass $m_{J/\psi K}$ and the kaon energy E_K. The signal distribution $S(m_{J/\psi K}, E_K)$ is modeled by a double-Gaussian function with six parameters, where both Gaussians have the same mean but different widths. The widths have an exponential dependence on E_K. Signal parameters are allowed to differ for the $\eta < -0.1$ and $\eta > 0.1$ regions to account for slight differences in the magnetic field along the beam direction.

The background distribution $P(m_{J/\psi K}, E_K)$ describes $B^{\pm} \to J/\psi \pi^{\pm}$ events where the pion is assigned the kaon mass, creating an artificially high reconstructed $B^{\pm}$ mass. Distribution P is a reflection of S with the mean mass value shifted to account for the K/π mass difference and the widths scaled by a ratio of the mean mass values. Background distribution $T(m_{J/\psi K})$ describes partially reconstructed decays of type $B_x \to J/\psi h^{\pm} X$, which have reconstructed mass lower than the $B^{\pm}$ mass. Distribution T is empirically modeled using a threshold function with a floating inflection point and the slope

fixed from MC simulation [25, 26]. Finally, the background distribution $E(m_{J/\psi K}, E_K)$ describes combinatoric background and is modeled using an exponential function with three parameters, where the slope depends on E_K.

The unbinned fit minimizes LLH, the negative log of the likelihood function $\mathcal{L}_n$ summed over N selected $B^{\pm}$ candidates, each with weight w_n (defined below):

$$\text{(2)} \qquad\qquad \text{LLH} = -2 \sum_{n=1}^{N} w_n \ln(\mathcal{L}_n).$$

Here $\mathcal{L}_n$ is a function of the four probability density distributions, with each assigned sample fraction f_i and forward-backward asymmetry A_i. While systematic effects were studied, the A_i parameters were blinded by adding unknown random offsets. The likelihood $\mathcal{L}_n$ has 26 parameters and is normalized to 1:

$$\text{(3)} \qquad \begin{aligned} \mathcal{L}_n = \alpha(E_K)[&f_S(1 + q_{\text{FB}} A_S)S + f_P(1 + q_{\text{FB}} A_P)P \\ &+ f_T(1 + q_{\text{FB}} A_T)T] + f_E(1 + q_{\text{FB}} A_E)E, \end{aligned}$$

where $f_E = [1 - \alpha(E_K)(f_S + f_P + f_T)]$ and $\alpha(E_K)$ uses three parameters to describe the dependence of the sample fractions on E_K [25].

Asymmetries in the detector material and J/ψ or $K^{\pm}$ reconstruction between $\eta < 0$ (the "north" side of the detector) and $\eta > 0$ (the "south" side) can result in an apparent A_{FB}. A north-south asymmetry is defined as $A_{\text{NS}} = (N_N - N_S)/(N_N + N_S)$. Because B^+ and B^- particles on the same side of the detector have opposite q_{FB}, corrections for north-south efficiency differences will generally cancel when determining $A_{\text{FB}}(B^{\pm})$. We measure A_{NS} in data samples with no expected production asymmetries. Decays of $\phi \to K^+K^-$ are used to measure $A_{\text{NS}}(K^{\pm})$. Signal and background models are determined from MC simulation and a χ^2 minimization fit is performed simultaneously on north- and south-side data. We measure $A_{\text{NS}}(K^{\pm})$ in bins of leading kaon $|\eta|$; there is no significant dependence on p_T. Integrated over all $|\eta|$, $A_{\text{NS}}(K^+) = (0.39 \pm 0.22)\%$ and $A_{\text{NS}}(K^-) = (0.64 \pm 0.23)\%$.

We measure $A_{\text{NS}}(J/\psi)$ using prompt $J/\psi \to \mu^+\mu^-$ decays. J/ψ mesons with significant L_{xy} are generally from B decays which could exhibit a north-south asymmetry due to $A_{\text{FB}}(B^{\pm})$. To reduce the fraction of nonprompt J/ψ mesons to a negligible level we require the J/ψ L_{xy} significance to be less than 1.5. Background events under the peak from 2.9 to 3.3 GeV are removed with a sideband subtraction, and $A_{\text{NS}}(J/\psi)$ is calculated in bins of $|\eta|$ and p_T. Integrated over all $|\eta|$ and p_T, $A_{\text{NS}}(J/\psi) = (-0.41 \pm 0.04)\%$.

Measured A_{NS} values are used to determine "efficiency weights" $w_{K\pm}$ and $w_{J/\psi}$ that equalize the relative reconstruction efficiencies on both sides of the detector. Applying these weights has a small effect on $A_{\text{FB}}(B^{\pm})$: a shift of 0.06% from $w_{K\pm}$ and a shift of -0.01% from $w_{J/\psi}$. Uncertainties on $A_{\text{NS}}(J/\psi)$ and $A_{\text{NS}}(K^{\pm})$ contribute an uncertainty of 0.003% to $A_{\text{FB}}(B^{\pm})$, determined using an ensemble test with 500 Gaussian variations of the A_{NS} values.

The total event weight is $w_n = w_{\text{magnet}} w_{K\pm} w_{J/\psi}$, where w_{magnet} equalizes the number of events in eight settings of solenoid polarity, toroid polarity, and $B^{\pm}$ charge. Equalizing the contribution from each magnet polarity combination removes tracking charge asymmetries to first order, since in one polarity a B^+ is reconstructed with the same sign of curvature as a B^- in the opposite polarity. Also equalizing the number of B^+
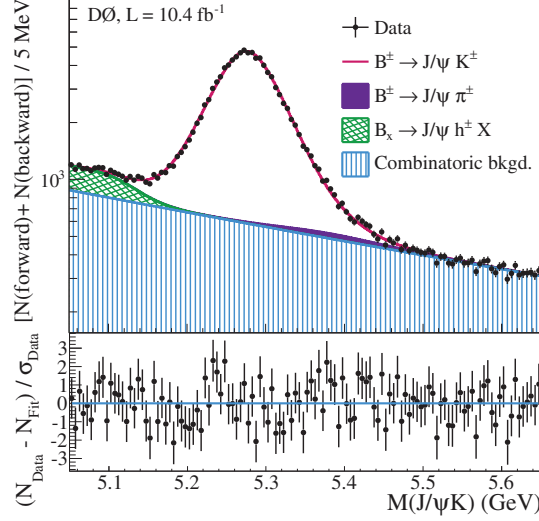
Fig. 1. – Invariant mass $M(J/\psi K)$ of (forward + backward) events with fitted distributions. The lower pane shows the residuals.
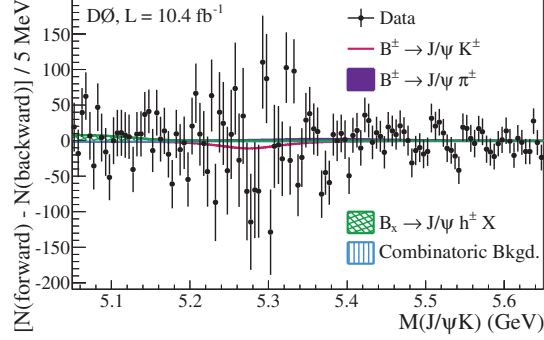

Fig. 2. – Invariant mass $M(J/\psi K)$ of (forward − backward) events with fitted distributions which include the asymmetry parameters A_i.

and B^{-} candidates eliminates the need to correct for different K^{+} and K^{-} interaction cross sections in the detector [27].

The weighted data sample contains $160\,360$ $B^{\pm}$ candidates and the fit yields $89\,328 \pm 349$ $B^{\pm} \rightarrow J/\psi K^{\pm}$ decays. Although the fit was unbinned, to visualize the data and fit quality, binned distributions of invariant mass $M(J/\psi K)$ for the sum and the difference in the numbers of forward and backward $B^{\pm}$ candidates with their projected fits are shown in figs. 1 and 2. Over both mass distributions we obtain $\chi^2/\text{ndf} = 249/214$. We measure a signal asymmetry consistent with zero: $A_{\text{FB}}(B^{\pm}) = [-0.24 \pm 0.41\,(\text{stat})]\%$. The asymmetry is consistent over time and with B^{+} and B^{-} samples fitted separately. Asymmetries of the background distributions are also consistent with zero.

To determine systematic uncertainties on $A_{\text{FB}}(B^{\pm})$ a number of variations are made to the analysis. Data sample variations include training four alternative BDTs with different variables or input samples and using a range of BDT discriminant cuts. Fit

TABLE I. – *Summary of uncertainties on $A_{FB}(B^{\pm})$ in data.*

Source	Uncertainty
Statistical	0.41%
Alternative BDTs and cuts	0.17%
Fit variations	0.06%
Reconstruction asymmetries	0.05%
Fit bias	0.02%
Systematic uncertainty	0.19%
Total uncertainty	0.45%

variations include varying the $B^{\pm}$ mass range, removing dependences on E_K from the distributions, allowing the slope of $T(m_{J/\psi K})$ to float, and fixing the background asymmetry parameters to zero.

To estimate the systematic error from the reconstruction asymmetries we measure $A_{\mathrm{NS}}(J/\psi)$ and $A_{\mathrm{NS}}(K^{\pm})$ using alternate data samples and calculations in different bins or with alternate fit parameters. Biases in the fitting procedure are explored with ensemble tests on randomized data, comparing input and fitted values of $A_{\mathrm{FB}}(B^{\pm})$. No bias is observed, and a systematic uncertainty is assigned based on the spread of results in the ensemble test. The total systematic uncertainty on the data measurement is 0.19%, as summarized in table I.

To compare this measurement to the SM, the MC@NLO simulation is analyzed as described above, applying $B^{\pm} \rightarrow J/\psi K^{\pm}$ selections and weights to correct for muon trigger effects. Additionally, reconstructed muon and kaon tracks must match tracks from generated $B^{\pm} \rightarrow J/\psi K^{\pm}$ decays. Since matching reconstructed and generated $B^{\pm}$ mesons leaves no background events, $A_{\mathrm{FB}}^{\mathrm{MC}}(B^{\pm})$ is calculated directly according to eq. (1).

The dominant systematic uncertainty on $A_{\mathrm{FB}}^{\mathrm{MC}}(B^{\pm})$ is due to renormalization and factorization energy scale choices. MC@NLO defines μ_R and μ_F for renormalization and factorization energy scales [15] as the square root of the average of $m_T^2 = m^2 + p_T^2$ for the b and $\bar{b}$ quarks [28], with b quark mass m set to 4.75 GeV. Since $A_{\mathrm{FB}}^{b\bar{b}}$ is zero at leading order, there is a large scale dependence in predictions at next-to-leading order [29]. Both scales are varied independently from $\frac{1}{2}\mu_{R,F}$ to $2\mu_{R,F}$ to estimate an uncertainty due to uncalculated higher orders. Half the largest spread of variations gives a systematic uncertainty of 0.44%. The uncertainty on $A_{\mathrm{FB}}^{\mathrm{MC}}(B^{\pm})$ due to b quark fragmentation is estimated by weighting events so the distribution of $p(B^{\pm})_{||}/p(b)$ matches a Bowler function [30] tuned to LEP data or SLD data, where $p(B^{\pm})_{||}$ is the component of $p(B^{\pm})$ in the b quark direction. Half the largest spread of variations to $A_{\mathrm{FB}}^{\mathrm{MC}}(B^{\pm})$ is 0.25%. The negligible PDF uncertainty of 0.03% is calculated by varying the twenty CTEQ6M1 eigenvectors by their uncertainties and determining the standard deviation of the variations. We find $A_{\mathrm{FB}}^{\mathrm{MC}}(B^{\pm}) = [2.31 \pm 0.34\,(\mathrm{stat}) \pm 0.51\,(\mathrm{syst})]\%$. Combining all data and MC uncertainties in quadrature, the MC@NLO result differs from data by $(2.55 \pm 0.76)\%$, or 3.3 standard deviations.

Figure 3 shows measurements of $A_{\mathrm{FB}}(B^{\pm})$ and $A_{\mathrm{FB}}^{\mathrm{MC}}(B^{\pm})$ *vs.* transverse momentum and pseudorapidity. The fully reconstructed $J/\psi K^{\pm}$ final state produces good kinematic
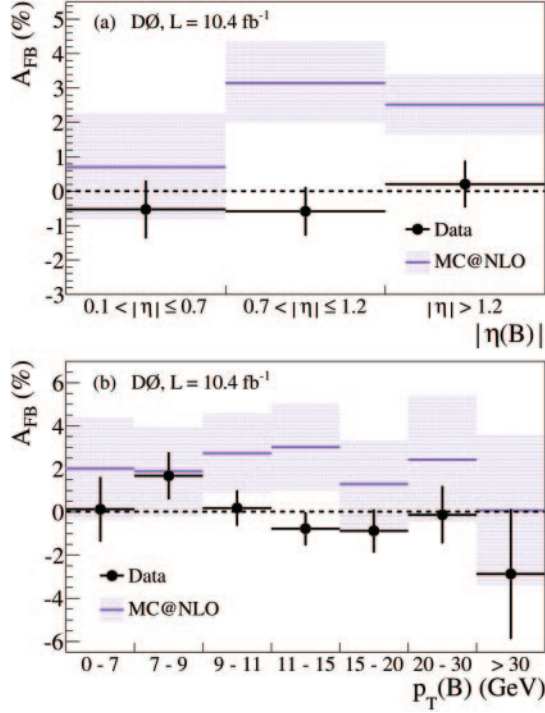
Fig. 3. – Comparison of $A_{\mathrm{FB}}(B^{\pm})$ and $A_{\mathrm{FB}}^{\mathrm{MC}}(B^{\pm})$ in bins of (a) $|\eta_B|$ and (b) $p_T(B)$. Data points and MC bands include statistical uncertainties convoluted with systematic uncertainties.

agreement between reconstructed and generated $B^{\pm}$ mesons, so corrections to recover the true $B^{\pm}$ kinematics are unnecessary. The average p_T of the $B^{\pm}$ mesons is 12.9 GeV. We find that $A_{\mathrm{FB}}(B^{\pm})$ is systematically lower than $A_{\mathrm{FB}}^{\mathrm{MC}}(B^{\pm})$ for all pseudorapidities, and for $p_T(B) = 9$–30 GeV. Considering the MC systematic uncertainties to be correlated (uncorrelated), fig. 3(a) has $\chi^2 = 10.3\,(11.8)$ for three bins and fig. 3(b) has $\chi^2 = 6.6\,(7.0)$ for seven bins.

In conclusion, we have measured the forward-backward asymmetry in the production of $B^{\pm}$ mesons with $B^{\pm} \rightarrow J/\psi K^{\pm}$ decays in $p\bar{p}$ collisions at $\sqrt{s} = 1.96$ TeV. For $B^{\pm}$ mesons with a mean p_T of 12.9 GeV, the result is $A_{\mathrm{FB}}(B^{\pm}) = [-0.24 \pm 0.41\,(\mathrm{stat}) \pm 0.19\,(\mathrm{syst})]\%$, which is the first measurement of this quantity. We observe a discrepancy of ≈ 3 standard deviations between our measurement and the MC@NLO estimate but our results are in good agreement with the recent SM prediction.

$$* \ * \ *$$

REFERENCES

[1] ALMEIDA L., STERMAN G. and VOGELSANG W., *Phys. Rev. D*, **78** (2008) 014008; KÜHN J. H. and RODRIGO G., *JHEP*, **01** (2012) 063; AGUILAR-SAAVEDRA J. A., AMIDEI D., JUSTE A. and PEREZ-VICTORIA M., arXiv:1406.1798 (2014).

[2] ABAZOV V. M. *et al.* (D0 COLLABORATION), *Phys. Rev. D*, **84** (2011) 112005.

[3] AALTONEN T. *et al.* (CDF COLLABORATION), *Phys. Rev. D*, **83** (2011) 112003; **87** (2013) 092002; **88** (2013) 072003.

[4] GRESHAM M. I., KIM I.-W. and ZUREK K. M., *Phys. Rev. D*, **83** (2011) 114027; AGUILAR-SAAVEDRA J. A. and PEREZ-VICTORIA M., *JHEP*, **09** (2011) 097; KAMENIK J. F., SHU J. and ZUPAN J., *Eur. Phys. J. C*, **72** (2012) 2102.

[5] GRINSTEIN B. and MURPHY C. W., *Phys. Rev. Lett.*, **111** (2013) 062003; **112** (2014) 239901.

[6] IPEK S., *Phys. Rev. D*, **87** (2013) 116010.

[7] ABAZOV V. M. *et al.* (D0 COLLABORATION), *Phys. Rev. D*, **87** (2013) 011103(R); **88** (2013) 112002; *Phys. Rev. D*, **90** (072011) 2014.

[8] BERNREUTHER W. and SI Z.-G., *Phys. Rev. D*, **86** (2012) 034026; CZAKON M., FIEDLER P. and MITOV A., arXiv:1411.3007 (2014).

[9] CHATRCHYAN S. *et al.* (CMS COLLABORATION), *JHEP*, **04** (2014) 191.

[10] AAD G. *et al.* (ATLAS COLLABORATION), *JHEP*, **02** (2014) 107.

[11] AAIJ R. *et al.* (LHCB COLLABORATION), *Phys. Rev. Lett.*, **113** (2014) 082003.

[12] ABAZOV V. M. *et al.* (D0 COLLABORATION), *Phys. Rev. Lett.*, **114** (2015) 051803.

[13] KÜHN J. H. and RODRIGO G., *Phys. Rev. D*, **59** (1999) 054017.

[14] MANOHAR A. V. and TROTT M., *Phys. Lett. B*, **711** (2012) 313.

[15] FRIXIONE S. and WEBBER B. R., *JHEP*, **06** (2002) 029; FRIXIONE S., NASON P. and WEBBER B. R., *JHEP*, **08** (2003) 007.

[16] PUMPLIN J. *et al.*, *J. High Energy Phys.*, **07** (2002) 012; STUMP D. *et al.*, *JHEP*, **10** (2003) 046.

[17] CORCELLA G., *JHEP*, **01** (2001) 010.

[18] BRUN R. and CARMINATI F., CERN Program Library Writeup W5013, 1993.

[19] MURPHY C. W., arXiv:1504.02493 (2015).

[20] ABAZOV V. M. *et al.* (D0 COLLABORATION), *Nucl. Instrum. Methods A*, **565** (2006) 463.

[21] ABAZOV V. M. *et al.*, *Nucl. Instrum. Methods A*, **552** (2005) 372; ABAZOV V. M. *et al.* (D0 COLLABORATION), *Nucl. Instrum. Methods A*, **737** (2014) 281.

[22] OLIVE K. A. *et al.* (PARTICLE DATA GROUP), *Chin. Phys. C*, **38** (2014) 090001.

[23] HOECKER A. *et al.*, Toolkit for multivariate Data Analysis, *Proc. Sci. ACAT* (2007) 040.

[24] SJÖSTRAND T., MRENNA S. and SKANDS P., *JHEP*, **05** (2006) 026.

[25] ABAZOV V. M. *et al.* (D0 COLLABORATION), *Phys. Rev. Lett.*, **110** (2013) 241801.

[26] ABAZOV V. M. *et al.* (D0 COLLABORATION), *Phys. Rev. D*, **87** (2013) 072006.

[27] ABAZOV V. M. *et al.* (D0 COLLABORATION), *Phys. Rev. D*, **86** (2012) 072009; **82** (2010) 032001.

[28] FRIXIONE S., (private communication).

[29] CAMPBELL J. M. and ELLIS R. K., FERMILAB-PUB-12-078-T (2012).

[30] CORCELLA G. and DROLLINGER V., *Nucl. Phys. B*, **730** (2005) 82.